JOURNAL OF SOLID STATE CHEMISTRY 77, 48–53 (1988)

IR and Visible Absorption Studies on $KNiBr_3$ Crystals

SHANKER RAM

Advanced Centre for Materials Science, IIT Kanpur 208016, India

AND KANIK RAM

DMSRDE, P.O. Box 320, Kanpur 208013, India

Received November 12, 1987; in revised form April 25, 1988

The absorption bands caused by the phonon vibrations and the $Ni^{2+}(3d^8)$ electronic transitions observed in $KNiBr_3$ single crystals have been studied. The Ni^{2+} ions in the present crystals appear to exist in a moderate octahedral coordination site [forming the $Ni(Br)_6$-type polyhedron] which is excited in the electronic as well as in the vibration (IR) spectrum. The electronic spectrum for some of the *d–d* transitions indicates well-resolved vibronic structures, the frequencies of which are consistent with those observed in the IR spectrum. © 1988 Academic Press, Inc.

1. Introduction

The ABX_3 (X for halogen) series of compounds, where A and B respectively refer to an alkali and a divalent transition/IIA group cation, is of interest for the laser hosts and/or for studying the imperfection centers (*1–4*). The optical absorption and luminescence spectra of the host and/or doped Ni/Co cations in the various ABF_3 fluoride crystals have been reported in this series (*2, 3*). However, few studies have been carried out on the other halides. We report here the electronic ($3d^8 \rightarrow 3d^8$) absorption spectra of possible $Ni^{2+}(d^8)$ centers in $KNiBr_3$ crystals. The results are discussed in the light of vibrational analysis proposed for the crystal vibration modes.

2. Experimental

The single crystals of $KNiBr_3$ investigated in this work were obtained from slow evaporation of an aqueous solution containing KBr and $NiBr_2$ in stoichiometric amounts. The formation of $KNiBr_3$ in the solution is confirmed by X-ray diffractometry of the crystal particles (using a Rich and Seifert-Isodebyeflex 2002 diffractometer with filtered Cu$K\alpha$ radiation) which indicates sharp and intense diffraction lines (Fig. 1) in the range $20° \leq 2\theta \leq 50°$. The data characteristically differ from those of $NiBr_2$ (*5a*) or KBr (*5b*) and $KNiX_3$ (X = F, Cl) halides (*5c, 5d*). The latter halides crystallize essentially in a hexagonal or cubic crystal system. The crystal structure of $KNiBr_3$ is believed to be monoclinic (space group C^3_{2h}, $Z = 2$), with the Ni^{2+} cation situated at an octahedral coordination site forming the $Ni(Br)_6$-type polyhedron. Other crystallographic details for $KNiBr_3$ remain to be determined.

IR spectra of the sample (ground into powder) were recorded on a Perkin–Elmer 783 spectrophotometer using a resolution of

0022-4596/88 $3.00

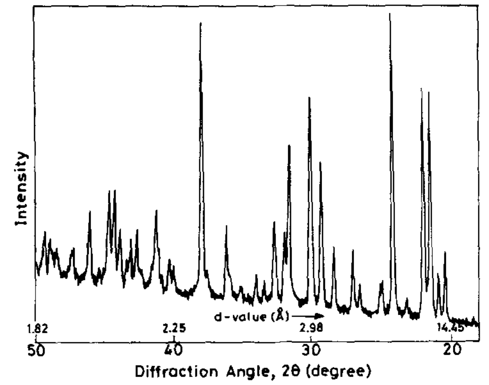

FIG. 1. X-ray powder diffraction patterns for $KNiBr_3$.

1.2 cm^{-1}. The measurements in the near IR and visible regions (2500–400 nm) were performed with thin polished platelet samples on a Cary 2300 spectrophotometer.

3. Results and Discussion

3.1 Phonon Vibrations

The IR spectrum of the sample (shown in Fig. 2) comprises a series of band groups in the region extending from 300 to 4000 cm^{-1}. The prominent bands lying below the 1200-cm^{-1} region could be correlated with the four expected fundamental modes, viz., ν_1, ν_2, ν_3, and ν_4 for $KNiBr_3$ crystal in perovskite-type structure (*6, 7*). The assignments of the individual bands observed in the spectrum are given in Table I.

TABLE I

PHONON BANDS (FUNDAMENTAL) OBSERVED IN THE IR SPECTRUM OF $KNiBr_3$

Frequency (cm^{-1})	Intensity (arb. units)	Assignment
370^s(a)	71	$\nu_4(E)$
420 (b)	Sh	
400 (a′)	67	
447 (b′)	Sh	
470 $(a)^s$	58	$\nu_2(A_1)$
535 (b)	75	
580 (a)	94	$\nu_1(A_1)$
620 (b)	99	
642 (a)	100	$\nu_3(E)$
770 (b)	95	
858 (a′)	80	
900 (b′)	75	
992^s	90	Electronic $Ni^{2+}\{^3F_4(\Gamma_3)\}$ bands
1125^a	100	

Note. s, sharp; Sh, shoulder bands. The modes ν_1, ν_3 represent stretching and ν_2, ν_4 the deformation modes in a moderate $Ni(Br)_6$ octahedron. The bands (corresponding to transverse and longitudinal modes) are marked by a and b, respectively.

[a] Overlapping bands make placement difficult.

It is logical to compare the results with those reported for the ideal ABY_3 perovskite (cubic crystal structure) with

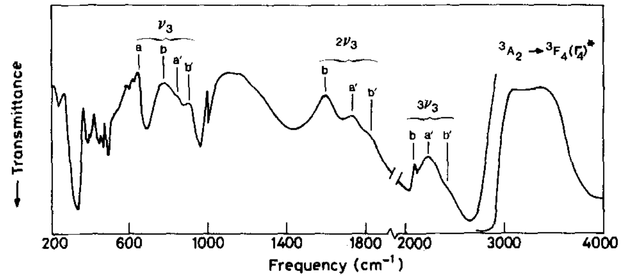

FIG. 2. IR spectrum of $KNiBr_3$ in KBr pellet. a, b, a′, and b′ refer to band components in ν_3 vibration mode and corresponding higher harmonic modes excited in the system. *Much intense electronic absorption because of Ni^{2+}. This could be recorded by reducing the vertical (transmittance) scale by a factor of 10.

space group $P_{m3m}(O_h^1)$ (*8*). The frequencies assigned for ν_1 and ν_3 vibrations in the present work are reasonably high and show a larger number of band components than expected even after the triplet degeneracy of T_{1u} and T_{2u} modes (cf. Table II) is lifted. One perspective is that the perovskite structure is probably distorted in $KNiBr_3$ crystals. The relationship involves a tetragonal distortion of the perovskite unit cell, together with a transition from an octahedral $Ni(Br)_6$ unit to tetrahedral $Ni(Br)_4$ by the shortening of Ni–Br bonds. In this model the above vibrations would present large frequencies in the tetrahedral scheme, and the prominent IR intensities observed even in the case of highly symmetric vibrations are very likely. A correlation diagram summarizing the various vibration species and their selection rules in the two crystal systems is given in Table II.

The assignment proposed for the various fundamental vibration modes of $KNiBr_3$ in Table I seems consistent with the X-ray diffraction analysis, which reveals a possible monoclinic structure (space group C_{2h}^3, and $Z = 2$) for the system at room temperature (295 K). All four fundamental vibrations of $KNiBr_3$ may be allowed in IR under the approximation of this crystal system and for the nickel cation forming a moderately distorted [$Ni(Br)_6$ type] polyhedron in the crystal unit cell as expected for the nickel bromide (*5a, 9*).

TABLE II

CORRELATION DIAGRAMS[a]

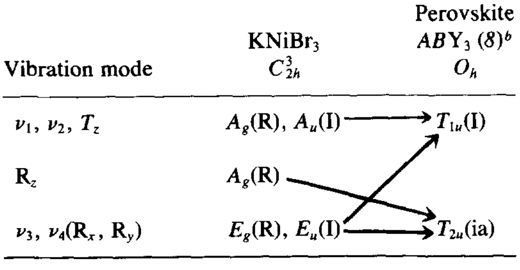

Vibration mode	KNiBr$_3$ C_{2h}^3		Perovskite ABY_3 (*8*)[b] O_h
ν_1, ν_2, T_z	A_g(R), A_u(I)	→	T_{1u}(I)
R_z	A_g(R)		
ν_3, ν_4(R_x, R_y)	E_g(R), E_u(I)	→	T_{2u}(ia)

[a] R, Raman active; I, infrared active; ia, inactive.

[b] There is no Raman active mode.

The site group symmetry for $Ni(Br)_6$ polyhedron in $KNiBr_3$ crystal is not known and therefore, with the data available at present, it is not possible to carry out a factor group analysis for the various vibrations. Also factor group splitting could not be resolved because a sharp band structure was lacking in the present spectrum. Moreover, all four fundamental vibrations are split into transverse and longitudinal components: TO/LO splitting (*10*). As a result, the number of bands in the spectrum is doubled by this TO/LO splitting. The corresponding bands are marked a and b, respectively, in Table I. The $E(\nu_3$ and $\nu_4)$ modes are further split into two distinct components by removal of the doublet degeneracy.

A sharp band observed at 992 cm^{-1} (Fig. 2) along with the broadband features centered at ~1125 cm^{-1} is believed to arise in $3d^8(Ni^{2+})$ electronic transitions excited to the crystal field splitant level (Γ_3) of the ground state multiplet $^3F_4$ (*11, 12*). The extension of the band features into the high-frequency side indicates mixing of the transition with lattice vibrations (not studied in the present work), thus resulting in the vibronic bands associated with the latter.

The band series showing unresolved triplet structures centered around 850, 1700, and 2250 cm^{-1} (cf. Fig. 2) have similar band profiles. The frequencies in those bands empirically follow the series $n\nu_3$, with $\nu_3 =$ 850 cm^{-1} and $n = 1 \rightarrow 3$. The intensity decreases successively in the series, confirming that the latter is due to the higher harmonics of ν_3 vibration. Similar harmonic bands have also been reported with measurable intensities up to $n = 4$ in $BaBiO_3$ perovskite (*13*).

3.2 Optical Transitions

The absorption spectrum of $KNiBr_3$ is shown in Fig. 3. The positions and intensi-

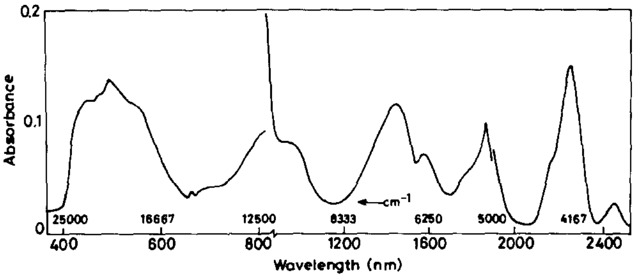

FIG. 3. Optical absorption spectrum of a $KNiBr_3$ crystal. The actual absorption in the region 800–400 nm is 10 times that shown on the vertical axis.

ties of the prominent bands together with the transitions assigned are summarized in Table III. The spectrum contains a group of characteristically broadbands which arise from the transitions within $3d^8(Ni^{2+})$ configuration.

The Ni^{2+} exhibits a series of $d \leftrightarrow d$ transitions occurring in the near IR to UV regions *(14)*. The transitions within these levels are in principle forbidden in the absorption. They usually appear, however, because of a coupling with the lattice vibrations. The resulting spectrum is very sensitive to coordination number, symmetry, and crystal field at the ion site offered by the nearest neighbors in the crystal. Absorption bands

TABLE III

ZERO PHONON LINES AND ASSOCIATED VIBRONIC TRANSITIONS OBSERVED IN THE OPTICAL ABSORPTION SPECTRUM OF $KNiBr_3$ CRYSTAL

Band position		Separation from zero phonon line	Assignment	
λ (nm)	ν (cm^{-1})	$\Delta\nu$ (cm^{-1})	(transitions $^3A_2 \rightarrow {}^3F, {}^1D, {}^3P$)	
3075	3252			$^3F_4(\Gamma_4)$
2450	4082	0	(0,0) band	
2243	4458	376	+ ν_4' (a)	$^3T_2\{^3F_3(\Gamma_5)\}$
2164	4620	539	+ ν_2' (b)	
1905	5249	0	(0,0) band	
1875	5333	84	?	$^3T_2\{F_3(\Gamma_2)\}$
1770	5650	401	+ ν_4' (a′)	
1570	6369	0	(0,0) band	$^3T_1\{^3F_4(\Gamma_1)\}$
1440	6944	575	+ ν_1' (a)	
1290	7752			$^3T_1\{^3F_3(\Gamma_4)\}$
940	10638			$^3T_1\{^1D_2(\Gamma_3), {}^3F_2(\Gamma_5)\}$
810	12345			
693	14430	0	(0,0) band	$^1E\{^3F_2(\Gamma_3)\}$
664	15060	630	+ ν_1' (b)	
579	17271			$^1T_2\{^1D_2(\Gamma_5)\}$
554	18050			
500	20000			$^3T_1\{^3P_{1,2}(\Gamma_{3,5,4})\}$
457	21882			

Note. ν_1', ν_2', etc., refer to the vibrations (Table I) associated with the excited electronic state.

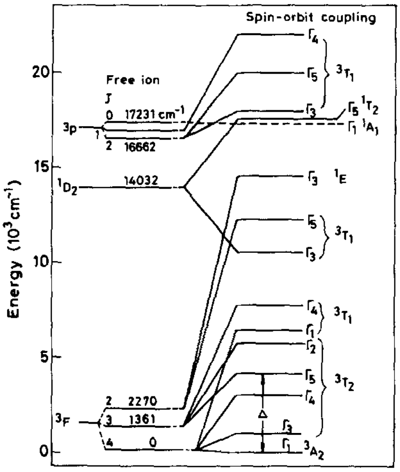

FIG. 4. Schematic splitting diagram of the $Ni^{2+}(d^8)$ levels adopted to the observed transitions for $KNiBr_3$ in moderate octahedral crystalline fields. Free ion energy values (cm^{-1}) and notations are taken from Ref. (*12*). The transition corresponding to $^3A_2(\Gamma_1) \rightarrow {}^3P_0$ level (shown by dotted line) was not observed in the present investigation.

corresponding to Ni^{2+} cations at both octahedral and tetrahedral coordination sites have been reported (*9, 11, 12, 14, 15*). Thus similar to the results for NiX_2 (*9, 15*) and $KNiX_3$ (other than X = Br) (*12*) halides, the spectrum of $KNiBr_3$ observed in the present investigation can be ascribed to the *d–d* transitions of Ni^{2+} in a moderate octahedral coordination.

The transitions from ground state $^3A_2(\Gamma_1)$ to the various levels of ground ($^3F_{3,2}$) and excited state (^3P, ^1D) multiplets are usually excited (cf. the assignments in Table III). The broad absorption with subsidiary maxima and satellite bands ranging from 8000 to 4000 cm^{-1} and below is assigned to transitions arising from the ^3F ground state multiplet. In Fig. 4 we show the various Ni^{2+} electronic energy levels as deduced from the observed absorption corresponding to zero phonon lines. The ^3F multiplet is split into two triplets ($^3T_1$ and $^3T_2$) and a singlet ($^3A_2$) because of crystalline field effects. The $^3A_2(\Gamma_1)$ is the lowest energy level (ground state) for the Ni^{2+} ions in an octahedral coordination site. It remains singlet even after the spin–orbit coupling. Also, the ligand field splitting of ^3F multiplet ($\Delta \sim$ 4100 cm^{-1}) is comparable with the spin–orbit splitting (~3250 cm^{-1}). In fact, a complicated splitting pattern of the ground state multiplet can be anticipated. Obviously, the zero phonon lines in the transitions originating from $^3A_2$ (e.g., cf. the bands at 4300 and 7000 cm^{-1}) are identified by the relatively sharper band edge on the lower energy side of the absorption maxima. These are further accompanied by several vibronic bands in the higher energy side, indicating that the transitions are allowed by vibration coupling. The vibrational structure, however, is obscured in most cases because of Jahn–Teller distortions in the degenerate states.

Some of the assignments of Ni^{2+} transitions indicated in Table III are still being discussed in the literature. For example, a transition $^3A_2 \rightarrow {}^1D_2(\Gamma_3)$ is not reported to appear in the spectrum of $KNiF_3$ (*12*). DeKock and Gruen (*15*) have assigned it to a sharp band at ~11500 cm^{-1} in $NiCl_2$. We agree with this assignment and accordingly have correlated a weak band observed at ~10638 cm^{-1} in $KNiBr_3$ to this transition. The comparatively diffuse band feature shown in the present case indicates a reasonably lower symmetry for the Ni^{2+} cations in $KNiBr_3$ crystal lattice.

A more interesting observation is that the electronic transitions of Ni^{2+} (except $^3A_2 \rightarrow {}^3T_1{}^1D_2(\Gamma_3)$) in $KNiBr_3$ comprise the considerably smaller energy values compared to those reported for $KNiF_3$ crystals (*12*). The latter crystallizes in a cubic crystal structure with Ni^{2+} located at the octahedral coordination site (O_h symmetry). Moreover, most of the transitions of $KNiBr_3$ correspond very closely in transition energies to those observed for $NiBr_2$ (hexagonal crystal system) crystal. The coordination polyhedron of $NiBr_2$ is a distorted octahedron (*9*). The $Ni(Br)_6$ octahedron is more likely to be distorted in $KNiBr_3$ crystal, with a transition from the octahedral coordination site toward the tetrahedral site. The Ni^{2+} electronic levels could comprise the smaller energy values for the latter (*14*).

From the splitting patterns observed for the ^3F multiplet we assigned a speculative crystal field parameter value $\Delta = 4100$ cm^{-1} to the nickel ion in an octahedral site. The value found in the present case is appreciably smaller than 6800 cm^{-1} reported for $KNiF_3$ crystals (*2, 12*) and shows good agreement with the value $\sim$4500 cm^{-1} proposed by DeKock and Gruen for $NiCl_2$ (*15*). This appears in accordance with the electronegative character of the F, Cl, and Br anions. Fluorine, being highly electronegative, could offer a stronger ligand field (larger Δ value) on the Ni^{2+} cations sites in the system.

The strongest absorption for the spectrum of $KNiBr_3$ is observed between 18,000 and 22,000 cm^{-1}. It frequently occurs in the nickel systems because of the transition of a 3*d* electron on the molecular orbital of the $Ni(Br)_6$ polyhedron unit, corresponding to a transfer of charge from the central ion to the ligands (*12, 14*).

References

1. W. A. Sibley and N. Koumvakalis, *Phys. Rev. B* **14,** 35 (1976).

2. A. T. Abdalian and P. Moch, *J. Appl. Phys.* **49,** 2189 (1978).

3. A. T. Abdalian, J. Cibert, and P. Moch, *J. Phys. C* **13,** 5587 (1980).

4. J. Danko, D. Pacheco, and B. DiBartolo, *J. Luminesc.* **28,** 27 (1983).

5. JCPDS File Nos. (*a*) 24.789, (*b*) 4.531, (*c*) 21.1002, and (*d*) 4.85.

6. Y. Khan, K. Nahm, M. Rosenberg, and H. Wiliner, *Phys. Status Solidi A* **39,** 79 (1977).

7. A. Viste and D. E. Irish, *Canad. J. Chem.* **55,** 3218 (1977).

8. W. G. Fateley, F. R. Dollish, N. T. McDevitt, and F. F. Bentley, "Infrared and Raman Selection Rules for Molecular and Lattice Vibrations: The Correlation Method," Wiley–Interscience, New York (1972).

9. Van A. Ludi and W. Feitknecht, *Helv. Chim. Acta.* **46,** 2226 (1963).

10. G. Turrel, "Infrared and Raman Spectra of Crystals," p. 176, Academic Press, New York/London (1972).

11. E. I. Zoroatskaya, B. Z. Malkin, A. L. Stolov, and Zh. S. Yakovleva, *Sov. Phys. (Solid State)* **10,** 255 (1968).

12. J. Ferguson, H. J. Guggenheim, and D. L. Wood, *J. Chem. Phys.* **40,** 822 (1964).

13. S. Tajima, S. Uchida, A. Masaki, H. Takagi, K. Kitazawa, and S. Tanaka, *Phys. Rev. B* **35,** 696 (1987).

14. G. Roussos and H. J. Schulz, *Phys. Status Solidi B* **100,** 577 (1980).

15. C. W. DeKock and D. M. Gruen, *J. Chem. Phys.* **44,** 4387 (1966).